Plasma Physics and Controlled Fusion

PAPER

Structured targets for advanced laser-driven sources

To cite this article: L Fedeli *et al* 2018 *Plasma Phys. Control. Fusion* **60** 014013

IOP Publishing Plasma Physics and Controlled Fusion
Plasma Phys. Control. Fusion **60** (2018) 014013 (8pp) https://doi.org/10.1088/1361-6587/aa8a54

Structured targets for advanced laser-driven sources

L Fedeli[1], **A Formenti**[1], **L Cialfi**[1], **A Sgattoni**[2,3], **G Cantono**[4,5,6,7] **and M Passoni**[1]

[1] Dipartimento di Energia, Politecnico di Milano, Italy
[2] LULI-UPMC: Sorbonne Universities, CNRS, École Polytechnique, CEA, F-75013 Paris, France
[3] LESIA, Observatoire de Paris, CNRS, UPMC: Sorbonne Universities, F-92195 Meudon, France
[4] LIDYL, CEA, CNRS, Universit Paris-Saclay, CEA Saclay, F-91191 Gif-sur-Yvette, France
[5] Universit Paris Sud, Paris, F-91400 Orsay, France
[6] National Institute of Optics, National Research Council (CNR/INO) A.Gozzini unit, I-56124 Pisa, Italy
[7] Enrico Fermi Department of Physics, University of Pisa, I-56127 Pisa, Italy

E-mail: luca.fedeli@polimi.it

Received 26 June 2017, revised 8 August 2017
Accepted for publication 4 September 2017
Published 6 November 2017

Abstract

Structured targets offer great control over ultra-intense laser-plasma interaction, allowing the optimization of laser-target coupling for specific applications. By means of particle-in-cell simulations we investigated three applications in particular: high-order harmonic generation (HHG) with grating targets, enhanced target coupling with multilayer targets and the generation of intense laser-driven terahertz (THz) pulses with structured targets. The irradiation of a solid grating target at the resonance angle for surface plasmon excitation enhances the HHG with respect to flat targets. Multilayer targets consisting of solid foils coated with a very low-density near-critical layer lead to a strong laser absorption and hot electron production that can improve laser-driven ion acceleration. We also explored the generation of THz radiation showing how using either gratings or multilayer targets the emission can be strongly enhanced with respect to simple flat targets.

Keywords: relativistic laser-plasma interaction, high-order harmonic generation, structured targets, laser-driven ion acceleration, laser-driven terahertz generation, particle-in-cell simulations

(Some figures may appear in colour only in the online journal)

1. Introduction

The realization of laser-driven ultra-intense radiation sources is one of the main goals of the research activities carried out in the field of relativistic laser–matter interaction. Various schemes have been proposed for a number of applications, including high-energy particle sources (electrons [1] and ions [2, 3]), high intensity photon sources [4], high-order harmonic generation (HHG) [5] and ultra-intense terahertz (THz) sources [6]. In parallel with the development of these applications, several advanced target concepts [7] have been investigated, aiming at an improvement or a better control over the aforementioned schemes.

In this work we review some recent numerical results obtained with two specific advanced targets: relativistic surface-plasmon enhanced HHG with gratings [8](section 2), electron heating and enhanced ion acceleration with multilayer targets [9–11](section 3). Moreover, we provide an exploratory numerical investigation of laser-driven THz generation exploiting the aforementioned target concepts (section 4). THz emission from solid targets irradiated at relativistic or sub-relativistic intensities has been correlated with the conversion efficiency of laser energy into hot electrons energy [12]. Since both grating targets [13, 14] and multilayer targets [11, 15] generally provide a significantly higher laser absorption with respect to simple flat targets, an enhancement of THz emission may also be expected.

2. Enhanced HHG with grating targets

Grating targets have been investigated for a wide variety of applications, including laser-driven ion acceleration [13, 14, 16], synchrotron emission [17], electron acceleration [18, 19] and control [20, 21] or enhancement [8, 22–25] of HHG from laser–solid interaction. Here we review a recent numerical work on HHG using solid grating targets, where we observed that the irradiation of a grating at the resonance angle for surface plasmon excitation enhances HHG with respect to a flat solid target [8].

HHG with relativistic laser pulses interacting with solid targets [5, 26–30] is due to the relativistic motion of the electrons in the intense laser field at the target surface [31, 32] and has been proposed as a way to achieve higher intensities of the emitted harmonics with respect to conventional schemes based on atomic recollision in gaseous targets [33]. Indeed, HHG generation with gas targets is ultimately limited by the ionization threshold ($I \sim 10^{15}$ W cm^{-2}), while such intensity limit does not apply for HHG with laser–solid interaction. The use of a grating as a target for HHG has been proposed as a strategy to angularly separate the emitted harmonics, in order to obtain a quasi-monochromatic extreme ultra-violet (XUV) source [24, 25, 34] (the harmonic orders between the 8th and the 80th of a Ti:Sapphire laser with a wavelength ~800 nm lie in the XUV spectral region). Given a grating with a spacing d between the grooves, the mth harmonic order is diffracted according to [21, 22]:

$$n\lambda/md = \sin(\theta_i) + \sin(\theta_{mn}), \tag{1}$$

where λ is the laser wavelength, n is the diffraction order, θ_i is the angle of incidence of the laser pulse and θ_{mn} is the diffraction angle.

When focusing a laser pulse on a grating target, a surface plasmon can be excited if a matching condition between the grating period and the angle of incidence is met. Experimental evidence of the excitation of surface plasmons in laser-grating interaction at relativistic intensities has been recently provided [13, 19, 35]. Since surface plasmon excitation is associated with electromagnetic field enhancement at the target surface, an enhancement of HHG can be expected, in addition to the grating diffraction effects.

Neglecting relativistic effects, for a cold, dense plasma (i.e. plasma frequency $\omega_p \gg 2\pi c/\lambda$), the resonance angle θ_{res} for surface plasmon excitation is given by [36]:

$$j\lambda/d = 1 + \sin(\theta_{res}), \tag{2}$$

where j is an integer. Even though equation (2) has been derived in a purely non-relativistic theory, recent works [13, 19, 35] suggest that this condition should hold even at relativistic laser intensities.

The irradiation of a grating target in a configuration suitable for the excitation of surface plasmons has been considered in [8], by means of 2D numerical simulations performed with the open source particle-in-cell (PIC) code *piccante* [37, 38]. A box size of $80\lambda \times 80\lambda$ and a resolution up to $\lambda/400$ were used. The laser had a normalized intensity $a_0 = 15$ and a temporal duration of 12 λ/c (intensity FWHM). The target was a 1λ thick grating with a spacing $d = 2\lambda$, which according to equation (2) corresponds to a resonance angle $\theta_{res} = 30°$. The peak-to-valley depth of the grooves was 0.25λ. A simple flat target was also simulated for comparison. The electron density of the targets was $n_e = 128 n_c$, sampled with 144 macro-particles per cell ($n_c = \frac{\pi m_e c^2}{\lambda^2 e^2}$ is the critical electron density (e is the elementary charge, m_e is the electron rest mass and c is the speed of light). In the simulations the targets were irradiated at various incidence angles (15°–45°) and a Fourier transform of the diffracted electromagnetic field was performed in order to extract the harmonic content.

Figure 1(a) shows the $\hat{z}$ component of the magnetic field before and after the interaction with the grating target. Figure 1(b) shows the Fourier transform of the $\hat{z}$ component of the magnetic field in the $x > 0$ half-plane for a flat target irradiated at 45° and for a grating target irradiated at $\theta_i = 15°, 30°, 35°$ and 45°. In the case of a flat target all the harmonic orders are emitted along the specular direction, while for the grating high-order harmonics are diffracted, according to equation (1). A strong enhancement of harmonic emission is observed at incidence angles close to 30°, the expected surface plasmon resonance angle, in particular for harmonic orders diffracted close to the target surface ($k_x = 0$).

Finally, figure 1(c) shows a comparison between the spectrum of the emission collected within 45° ± 2.5° for the flat target irradiated at 45° and that of the emission collected within 80° ± 2.5° for the grating target irradiated at 35° (these cases were observed to provide the highest harmonic yield for the two target types). While the spectrum for the flat target is dominated by the $m = 1$ order (i.e. the reflected laser light), for the grating a suppression of the $m = 1$ order and a significant increase of the intensity of emitted harmonics is observed. The enhancement of the harmonic emission is particularly evident for higher harmonic orders (≈2 orders of magnitude for $m = 40$).

These results show that the implementation of the described scheme in a laser-plasma interaction experiment should allow to observe higher-order harmonics irradiating a grating target near-resonance than a simple flat target. This approach may find application as an ultra-intense, quasi-monochromatic, XUV source.

3. Foam-attached foils for enhanced electron heating and ion acceleration

Multilayer targets consisting in solid foils coated with a low-density layer [39–41] have been investigated within the framework of laser-driven ion acceleration [2, 3], where they have been proven to optimize the process. Specifically, they can lead to an increase of both the energy and the number of accelerated ions with respect to flat solid foils [9–11, 15, 41–43]. This could be beneficial for several potential applications [44, 45], such as radiotherapy [46, 47], material science [48, 49] or ultra-fast neutron sources [50].

Here we review some recent results concerning a numerical investigation of electron heating with multilayer targets [11], which is strongly related to the ion acceleration process [2, 3].

The use of a solid foil coupled with a low-density layer—near-critical when fully ionized—has been proposed as a

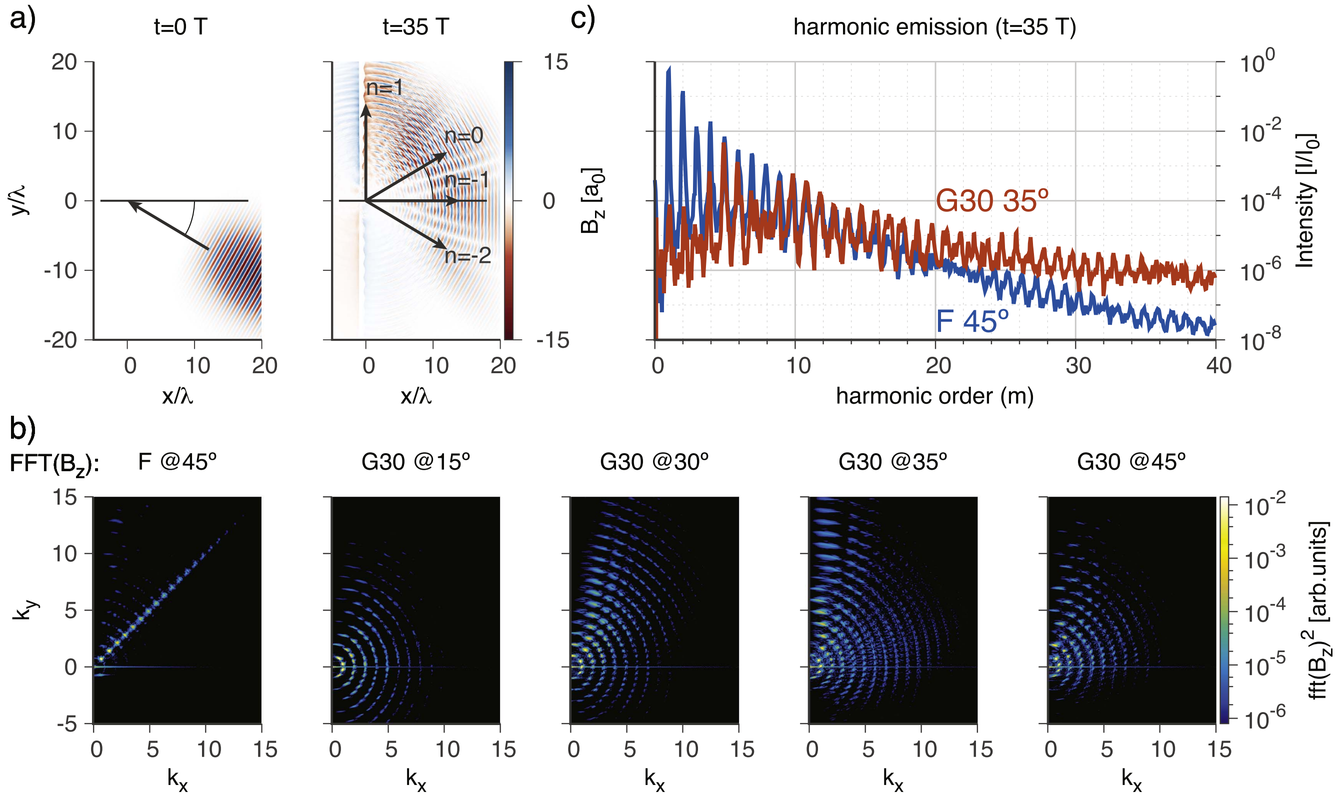

Figure 1. Resonant enhancement of HHG with grating targets. (a) $\hat{z}$ component of the magnetic field before and after the interaction with the grating target (expected resonance at 30°). (b) Fourier transform of B_z for a flat target irradiated at 45° and for the grating target irradiated at 15°, 30°, 35°, 45°. (c) Spectrum of the emitted radiation collected by a synthetic detector at 45° ± 2.5° and 80° ± 2.5° for the grating target.

possible solution to increase laser-target coupling [15, 51]. Indeed, laser interaction with a plasma at density $n_e \sim n_c$ is characterized by strong absorption and several nonlinear effects such as channel formation [52], self-focusing [52] and high-energy particle acceleration [53].

Experimental and numerical investigations of laser-driven ion acceleration with near-critical materials [9, 10, 41–43] reported a strong enhancement of the energy and the number of accelerated ions under certain target parameters. In [9, 10, 43] the effect was attributed to an enhanced target normal sheath acceleration (TNSA) mechanism due to an increase of the energy and of the number of electrons accelerated towards the back side of the target, while in [41] authors claimed an enhanced radiation pressure acceleration mechanism due to self-focusing and steepening of the laser pulse in the near-critical plasma.

Near-critical layers in [9, 10, 43], were obtained coating a thin solid foil with a very low-density nanostructured carbon foam [40]), whereas in [41, 42] authors exploited nanotubes and plastic foams, respectively. Regardless of the technique, while near-critical on average, all these targets are constituted by alternating voids and solid-density nanostructures. Due to the extreme contrast of modern day ultra-short laser systems [54], these nanostructures can survive long enough to influence the interaction with the laser.

In [11] an extensive numerical campaign was carried out in order to elucidate the electron heating process in multilayer targets, taking into account a possible role played by the nanostructure of the near-critical layer. In this work 2D numerical simulations were performed with *piccante* code [37, 38]. Simulated targets consisted in 0.5 μm thick pre-ionized ($Z/A = 1/3$) foils with an electron density $n_e = 80n_c$, coated with a 8 μm thick 'foam' layer with an average electron density equal to $1n_c$ ($Z/A = 1/2$). Two different types of foam were compared: a 'homogeneous' and a 'nanostructured' near-critical layer consisting in a spatially random collection of 10 nm over-dense (100 n_c) spheres, with a filling factor of 1% (so that the average density of the plasma was still 1 n_c). The laser pulse ($\lambda = 0.8\,\mu$m) was P-polarized, Gaussian shaped in the transverse direction (waist of 3 μm) with $\sin^2$ temporal envelope (intensity FWHM of 25 fs). The peak intensity was varied between the normalized laser amplitudes $a_0 = 1.5$ and $a_0 = 15$ (i.e. from a table-top multi-TW facility up to a few hundred s TW facility [55]). The angle of incidence was 30°. As reported in figure 2, laser interaction with foam-attached targets, either modelled with a homogeneous or nanostructured near-critical layer, results in an enhanced laser-matter coupling, leading to a significant increase of the electron temperature with respect to simple foils. The electron temperature was found to be lower for the nanostructured target than for the homogeneous one. This might be due to the fact that a fraction of the total energy is lost to the ion population in the Coulomb explosion of the nanospheres. A similar effect was observed in [56], where an extensive parametric investigation of laser interaction with

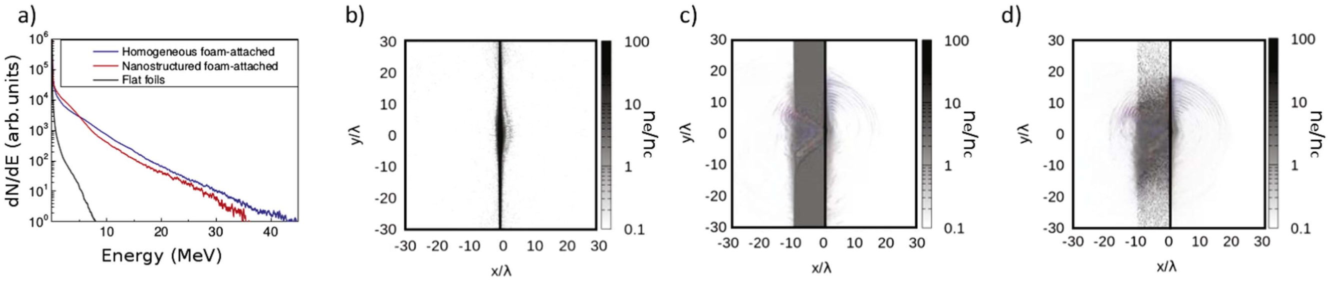

Figure 2. Laser interaction with flat foils and foam-attached targets. (a) Electron energy spectra taken when the kinetic energy of the electron population reaches its maximum for a flat foil (black), a nanostructured foam-attached target (red) and a homogeneous foam-attached target (blue). (b)–(d) Electron density normalized with respect to the critical density for a flat foil, homogeneous foam-attached target and nanostructured foam-attached target, respectively. The snapshots were taken at the same temporal frame of panel (a). The $\hat{z}$ component of the magnetic field is superimposed to the density plot in blue-red scale.

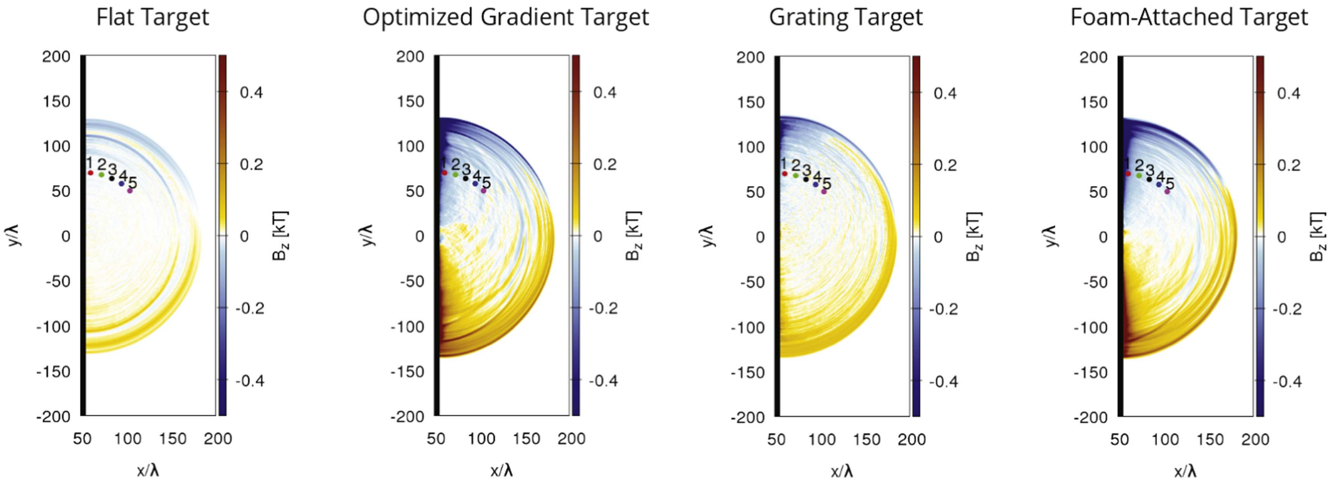

Figure 3. The B_z field component at $t = 200\lambda/c$ averaged over one laser cycle for the flat target, the target with an exponential density gradient optimized for resonant absorption, the grating target and the foam-attached target described in section 4. The numbered dots show the position of 'probe' diagnostics, which collect the value of the electromagnetic field as a function of time in a given position. Probes are positioned at a 70λ distance from the target centre, at 85°, 75°, 65°, 55° and 45° from target normal, respectively. Field intensities are shown in kiloTesla units (for the conversion from code units, a laser wavelength $\lambda = 0.8\ \mu$m was considered).

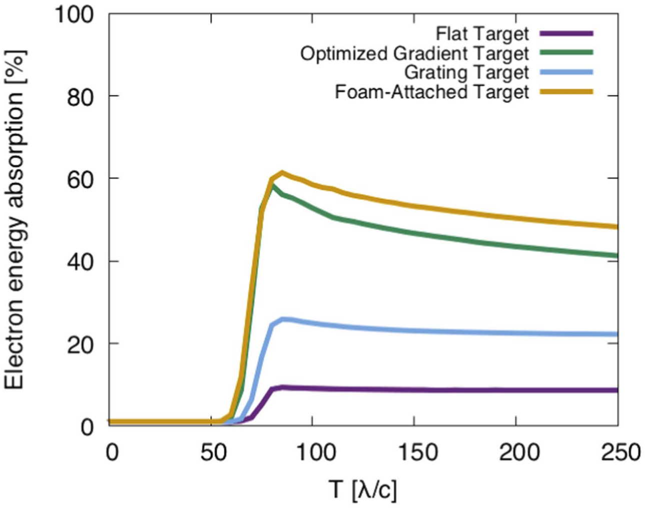

Figure 4. Absorption of laser energy into electron kinetic energy as a function of time for all the cases simulated in section 4. After reaching a peak at $t \approx 75\lambda/c$, the energy of the electron population decreases over time due to energy absorbed by the ion acceleration process.

nanostructured near-critical plasmas was carried out. In order to benchmark the results of this numerical campaign with experimental data, the electron temperatures obtained from the simulations were coupled with simple models of TNSA [57], providing an estimation for the maximum ion energies. Estimations obtained using the electron temperature of the nanostructured case proved to be in close agreement with recent experimental results [9, 10], while the higher temperatures obtained with the uniform foam targets lead to an overestimation of the ions maximum energies. The higher electron temperatures obtained with foam-attached targets with respect to simple flat foils justify the higher ion energies observed in the experiments with the formers.

We remark that simulations with foam-attached targets in [11] were performed with a relatively small angle of incidence of 30°. However, results in [15] provide an indirect indication that foam-attached targets could still allow for a significant enhancement of electron heating with respect to flat solid foils even for larger incidence angles (up to 60°).

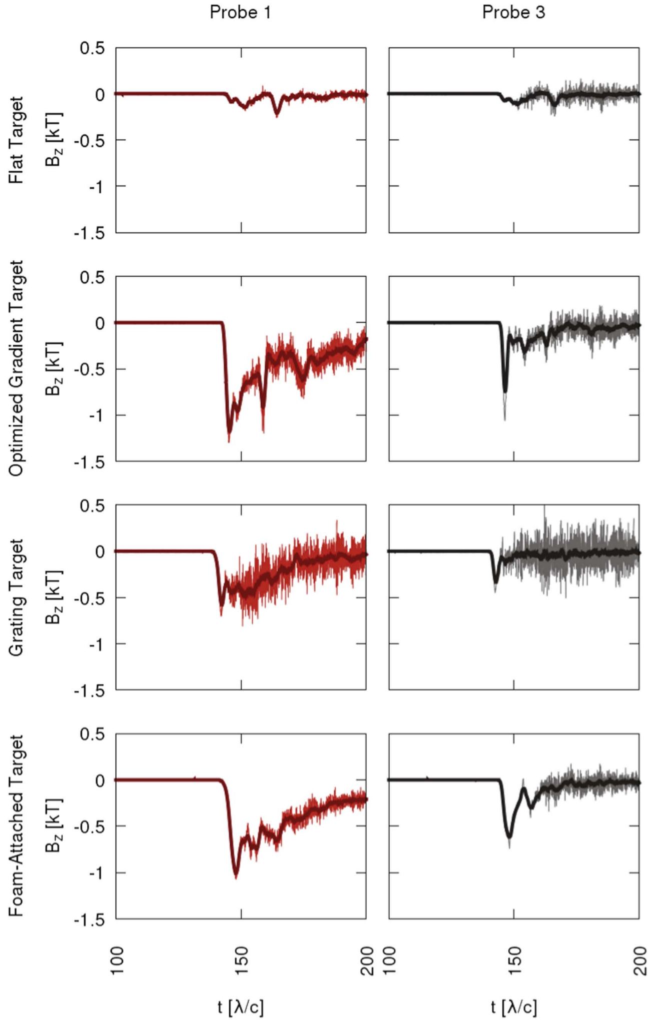

Figure 5. $\hat{z}$ component of the magnetic field as a function of time measured by probes 1 and 3 (see figure 3) for all the simulated targets. The light shade curves represent raw data, whereas the darker curves are calculated averaging over 120 neighbouring points (i.e. within a $\pm\, 0.86\lambda/c$ interval). Field intensities are shown in kiloTesla units (for the conversion from code units, a laser wavelength $\lambda = 0.8\ \mu$m was considered).

4. THz generation with structured targets

THz sources are of great interest for several scientific and technological applications [58, 59], such as time-resolved THz spectroscopy [60] or imaging [61]. Conventional THz sources with high energy per pulse (in the range of $\sim$100 μJ) are based on large electron accelerators [62, 63]. Recently, sources based on ultra-intense laser–solid interaction have been proposed as a possible path to generate THz pulses with energies similar to those that can be obtained with particle accelerators, but with a compact set-up [6, 12, 64–69]. The experimental observation of 400 μJ per pulse broadband THz emission from solid foils irradiated at $I \sim 10^{19}$ W cm^{-2} has been reported [6, 66], with a peak power of the emitted radiation approaching 1 GW [6]. THz emission from the rear of irradiated targets is attributed to coherent transition radiation of hot electrons [12, 65, 66, 70, 71], transient surface currents [6] and time varying TNSA charge separation field at the rear side of the target [6]. In these scenarios the intensity of THz emission has been directly correlated with the laser absorption. As already discussed, structured targets provide a mean to improve laser absorption [11, 13–15], which might also lead to an enhancement of THz emission. Here we present an exploratory numerical investigation of THz emission from irradiated gratings and multilayer targets. The properties of THz emission using these structured targets are compared with those obtained using a simple foil and a solid foil with a tailored exponential ramp (the gradient length-scale has been chosen so to enhance resonance absorption, as in [12]).

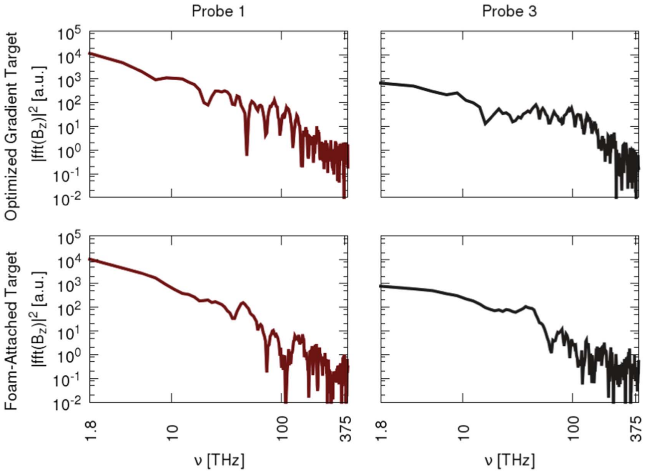

Figure 6. Squared amplitude of the Fourier transform of the $\hat{z}$ component of the magnetic field seen by probes 1 and 3. The lower limit of the frequency axis (1.8 THz) is due to the time window of the probe diagnostics. The laser frequency is ≈375 THz. Only data for the optimized gradient target and the foam-attached target are shown, since the strongest emission is observed in these cases.

Numerical simulations were performed with the open source, massively parallel PIC code *Smilei* [72]. In this section *Smilei* rather than *piccante* was used due to its additional diagnostics, such as 'probes' and time-averaged fields. Cross-checks were performed between the two codes showing a very good agreement. A $250\lambda \times 448\lambda$ numerical box with a resolution of 48 points per wavelength was used. The simulation time was $350\lambda/c$. The P-polarized laser pulse had a Gaussian transverse shape (waist of 5λ), a Gaussian temporal profile (field FWHM duration of $15\lambda/c$) and a normalized laser intensity of $a_0 = 2$ (i.e. a mildly relativistic regime accessible with a compact $\sim$10 TW laser system [14]). The incidence angle was 30°.

Four different targets were simulated: a simple flat foil (5λ thick, $n_e = 40n_c$), a grating target (5λ thick, $n_e = 40n_c$, 0.25 λ peak-to-valley depth, distance of the grooves $d = 2\lambda$), a foam-attached target (flat foil plus 5λ thick uniform foam layer at $n_e = 1n_c$) and a simple target with an exponential density ramp (5λ thick, $n_e = 40n_c$, length-scale of the ramp $l = 0.65\lambda$, which is the optimal length-scale for resonance absorption at 30° [73]). Forty-nine macro-electrons per cell were used to sample the electron density.

Figure 3 shows the $\hat{z}$ component (averaged over one laser cycle) of the magnetic field at $t = 200\lambda/c$ for the considered targets. In the four cases the emission of a half-cycle electromagnetic burst from the back side of the target can be observed. The lowest intensity of the emitted radiation is observed for the flat target. All the other targets allow for a significant enhancement of electromagnetic emission with respect to the former. The strongest emission is obtained with the gradient target and the foam-attached target. The intensity of this electromagnetic burst can be directly correlated with the conversion efficiency of laser energy into electron kinetic energy, reported in figure 4. The absorption efficiency is $\approx$10% for the flat target, while it reaches $\approx$20% for the grating target and $\approx$60% for the other two targets. Figure 5 shows the $\hat{z}$ component of the magnetic field measured by 'probes' 1 and 3 (see figure 3). The decay time of the signal is of the order of several tens of λ/c, which implies a typical frequency of few tens of THz for $\lambda = 0.8\ \mu$m.

Figure 6 shows the squared amplitude of the Fourier transform of the signal detected by probes 1 and 3 for the optimized gradient and the foam-attached targets. The signal is broadband between few THz and $\approx$100 THz. Limited differences can be observed in the spectra obtained with the two targets. These results confirmed that, as previously suggested [12], the THz emission from a target with a controlled plasma gradient is significantly higher than from a simple flat foil. The grating target allows for a moderate enhancement of the THz emission. On the other hand, using foam-attached targets the emission intensity is comparable with that obtained with the gradient target. However, foam-attached targets do not require a fine control of the laser temporal shape nor a pre-heating pulse in order to obtain a tailored gradient. This relaxes the experimental set-up, while still allowing for a significant THz emission.

5. Conclusions

Our results show that structured targets can be used to optimize laser-plasma coupling for a variety of applications. Here we have considered two specific target designs irradiated at laser intensities readily available in existing laser facilities: grating targets and foam-attached targets. Irradiating grating targets with an angle of incidence close to the one expected for surface plasmon resonance allows a significant enhancement of HHG with respect to simple flat targets. Foam-attached targets consisting of solid foils coated with a near-critical layer allow one to strongly enhance the laser-to-electrons conversion efficiency; this leads to an increase of the maximum energy and of the total charge of the TNSA ions. Finally, numerical simulations suggest that gratings and multilayer targets are a promising solution for the generation of electromagnetic bursts at THz frequencies, since in both cases a strong enhancement of THz emission with respect to simple flat targets is observed.

Acknowledgments

We gratefully thank Anna Grassi (Pierre et Marie Curie University, Paris and University of Pisa, Italy) for providing assistance in the use of *Smilei* PIC code.

The research leading to these results has received funding from the European Research Council Consolidator Grant ENSURE (ERC-2014-CoG No. 647554). We also acknowledge IscraC and LISA access schemes to MARCONI HPC machine at CINECA(Italy) via the projects LAST and SNAP.

References

[1] Esarey E, Schroeder C B and Leemans W P 2009 Physics of laser-driven plasma-based electron accelerators *Rev. Mod. Phys.* **81** 1229–85
[2] Daido H, Nishiuchi M and Pirozhkov A S 2012 Review of laser-driven ion sources and their applications *Rep. Prog. Phys.* **75** 056401
[3] Macchi A, Borghesi M and Passoni M 2013 Ion acceleration by superintense laser-plasma interaction *Rev. Mod. Phys.* **85** 751–93
[4] Sarri G *et al* 2013 Table-top laser-based source of femtosecond, collimated, ultrarelativistic positron beams *Phys. Rev. Lett.* **110** 255002
[5] Teubner U and Gibbon P 2009 High-order harmonics from laser-irradiated plasma surfaces *Rev. Mod. Phys.* **81** 445–79
[6] Gopal A *et al* 2013 Observation of gigawatt-class THz pulses from a compact laser-driven particle accelerator *Phys. Rev. Lett.* **111** 074802
[7] Prencipe I *et al* 2017 Targets for high repetition rate laser facilities: needs, challenges and perspectives *High Power Laser Sci. Eng.* **5**
[8] Fedeli L, Sgattoni A, Cantono G and Macchi A 2017 Relativistic surface plasmon enhanced harmonic generation from gratings *Appl. Phys. Lett.* **110** 051103
[9] Prencipe I *et al* 2016 Development of foam-based layered targets for laser-driven ion beam production *Plasma Phys. Control. Fusion* **58** 034019
[10] Passoni M *et al* 2016 Toward high-energy laser-driven ion beams: nanostructured double-layer targets *Phys. Rev. Accel. Beams* **19** 061301
[11] Cialfi L, Fedeli L and Passoni M 2016 Electron heating in subpicosecond laser interaction with overdense and near-critical plasmas *Phys. Rev.* E **94** 053201
[12] Ding W J and Sheng Z M 2016 Sub GV/cm terahertz radiation from relativistic laser–solid interactions via coherent transition radiation *Phys. Rev.* E **93** 063204
[13] Ceccotti T *et al* 2013 Evidence of resonant surface-wave excitation in the relativistic regime through measurements of proton acceleration from grating targets *Phys. Rev. Lett.* **111** 185001
[14] Blanco M, Flores-Arias M T, Ruiz C and Vranic M 2017 Table-top laser-based proton acceleration in nanostructured targets *New J. Phys.* **19** 033004
[15] Sgattoni A, Londrillo P, Macchi A and Passoni M 2012 Laser ion acceleration using a solid target coupled with a low-density layer *Phys. Rev.* E **85** 036405
[16] Bigongiari A, Raynaud M, Riconda C and Héron A 2013 Improved ion acceleration via laser surface plasma waves excitation *Phys. Plasmas* **20** 052701
[17] Pan K Q, Zheng C Y, Wu D, Cao L H, Liu Z J and He X T 2015 Study of strong enhancement of synchrotron radiation via surface plasma waves excitation by particle-in-cell simulations *Appl. Phys. Lett.* **107** 183902
[18] Raynaud M, Kupersztych J, Riconda C, Adam J C and Héron A 2007 Strongly enhanced laser absorption and electron acceleration via resonant excitation of surface plasma waves *Phys. Plasmas* **14** 092702

[19] Fedeli L *et al* 2016 Electron acceleration by relativistic surface plasmons in laser-grating interaction *Phys. Rev. Lett.* **116** 015001

[20] Yeung M, Zepf M, Geissler M and Dromey B 2011 Angularly separated harmonic generation from intense laser interaction with blazed diffraction gratings *Opt. Lett.* **36** 2333–5

[21] Cerchez M, Giesecke A L, Peth C, Toncian M, Albertazzi B, Fuchs J, Willi O and Toncian T 2013 Generation of laser-driven higher harmonics from grating targets *Phys. Rev. Lett.* **110** 065003

[22] Lavocat-Dubuis X and Matte J-P 2009 Numerical simulation of harmonic generation by relativistic laser interaction with a grating *Phys. Rev.* E **80** 055401

[23] Lavocat-Dubuis X and Matte J-P 2010 Numerical and theoretical study of the generation of extreme ultraviolet radiation by relativistic laser interaction with a grating *Phys. Plasmas* **17** 093105

[24] Zhang S J, Zhuo H B, Zou D B, Gan L F, Zhou H Y, Li X Z, Yu M Y and Yu W 2016 Model of high-order harmonic generation from laser interaction with a plasma grating *Phys. Rev.* E **93** 053206

[25] Pan K Q, Zheng C Y and He X T 2016 Surface plasma waves with their harmonics generation from pre-structured targets *Phys. Plasmas* **23** 023109

[26] von der Linde D, Engers T, Jenke G, Agostini P, Grillon G, Nibbering E, Mysyrowicz A and Antonetti A 1995 Generation of high-order harmonics from solid surfaces by intense femtosecond laser pulses *Phys. Rev.* A **52** R25–7

[27] Norreys P A *et al* 1996 Efficient extreme UV harmonics generated from picosecond laser pulse interactions with solid targets *Phys. Rev. Lett.* **76** 1832–5

[28] Bierbach J *et al* 2012 Generation of 10 μW relativistic surface high-harmonic radiation at a repetition rate of 10 Hz *New J. Phys.* **14** 065005

[29] an der Brügge D, Kumar N, Pukhov A and Rödel C 2012 Influence of surface waves on plasma high-order harmonic generation *Phys. Rev. Lett.* **108** 125002

[30] Kahaly S, Monchocé S, Vincenti H, Dzelzainis T, Dromey B, Zepf M, Martin P and Quéré F 2013 Direct observation of density-gradient effects in harmonic generation from plasma mirrors *Phys. Rev. Lett.* **110** 175001

[31] Baeva T, Gordienko S and Pukhov A 2006 Theory of high-order harmonic generation in relativistic laser interaction with overdense plasma *Phys. Rev.* E **74** 046404

[32] Quéré F, Thaury C, Monot P, Dobosz S, Martin P, Geindre J-P and Audebert P 2006 Coherent wake emission of high-order harmonics from overdense plasmas *Phys. Rev. Lett.* **96** 125004

[33] Paul A, Bartels R A, Tobey R, Green H, Weiman S, Christov I P, Murnane M M, Kapteyn H C and Backus S 2003 Quasi-phase-matched generation of coherent extreme-ultraviolet light *Nature* **421** 51–4

[34] Yeung M *et al* 2013 Near-monochromatic high-harmonic radiation from relativistic laser plasma interactions with blazed grating surfaces *New J. Phys.* **15** 025042

[35] Sgattoni A, Fedeli L, Cantono G, Ceccotti T and Macchi A 2016 High field plasmonics and laser-plasma acceleration in solid targets *Plasma Phys. Control. Fusion* **58** 014004

[36] Pitarke J M, Silkin V M, Chulkov E V and Echenique P M 2007 Theory of surface plasmons and surface-plasmon polaritons *Rep. Prog. Phys.* **70** 1

[37] Sgattoni A, Fedeli L and Sinigardi S Piccante: an open-source, fully relativistic, massively parallel particle-in-cell code http://aladyn.github.io/piccante/

[38] Sgattoni A, Fedeli L, Sinigardi S, Marocchino A, Macchi A, Weinberg V and Karmakar A 2015 Optimising PICCANTE—an open source particle-in-cell code for advanced simulations on Tier-0 systems (arXiv:1503.02464)

[39] Okihara S *et al* 2004 Ion generation in a low-density plastic foam by interaction with intense femtosecond laser pulses *Phys. Rev.* E **69** 026401

[40] Zani A, Dellasega D, Russo V and Passoni M 2013 Ultra-low density carbon foams produced by pulsed laser deposition *Carbon* **56** 358–65

[41] Bin J H *et al* 2015 Ion acceleration using relativistic pulse shaping in near-critical-density plasmas *Phys. Rev. Lett.* **115** 064801

[42] Willingale L *et al* 2009 Characterization of high-intensity laser propagation in the relativistic transparent regime through measurements of energetic proton beams *Phys. Rev. Lett.* **102** 125002

[43] Passoni M, Zani A, Sgattoni A, Dellasega D, Macchi A, Prencipe I, Floquet V, Martin P, Liseykina T V and Ceccotti T 2014 Energetic ions at moderate laser intensities using foam-based multi-layered targets *Plasma Phys. Control. Fusion* **56** 045001

[44] Najmudin Z, Fiuza F and Fernndez J C 2016 Summary of working group 6: ion acceleration with lasers *AIP Conf. Proc.* **1777** 030006

[45] Linz U and Alonso J 2016 Laser-driven ion accelerators for tumor therapy revisited *Phys. Rev. Accel. Beams* **19** 124802

[46] Bulanov S V, Zh Esirkepov T, Khoroshkov V S, Kuznetsov A V and Pegoraro F 2002 Oncological hadrontherapy with laser ion accelerators *Phys. Lett.* A **299** 240–7

[47] Amato E, Italiano A, Margarone D, Pagano B, Baldari S and Korn G 2016 Future laser-accelerated proton beams at eli-beamlines as potential source of positron emitters for PET *J. Instrum.* **11** C04007

[48] Hidding B *et al* 2017 Laser-plasma-based space radiation reproduction in the laboratory *Sci. Rep.* **7** 42354

[49] Barberio M, Veltri S, Scisciò M and Antici P 2017 Laser-accelerated proton beams as diagnostics for cultural heritage *Sci. Rep.* **7** 40415

[50] Alejo A, Ahmed H, Green A, Mirfayzi S R, Borghesi M and Kar S 2016 Recent advances in laser-driven neutron sources *Nuovo Cimento* C **38** 188

[51] Nakamura T, Tampo M, Kodama R, Bulanov S V and Kando M 2010 Interaction of high contrast laser pulse with foam-attached target *Phys. Plasmas* **17** 113107

[52] Pukhov A and Meyer-ter Vehn J 1996 Relativistic magnetic self-channeling of light in near-critical plasma: three-dimensional particle-in-cell simulation *Phys. Rev. Lett.* **76** 3975–8

[53] Gahn C, Tsakiris G D, Pukhov A, Meyer-ter Vehn J, Pretzler G, Thirolf P, Habs D and Witte K J 1999 Multi-MeV electron beam generation by direct laser acceleration in high-density plasma channels *Phys. Rev. Lett.* **83** 4772–5

[54] Thaury C *et al* 2007 Plasma mirrors for ultra-high intensity optics *Nat. Phys.* **3** 424–9

[55] Danson C, Hillier D, Hopps N and Neely D 2015 Petawatt class lasers worldwide *High Power Laser Sci. Eng.* **3** e3

[56] Fedeli L, Formenti A, Bottani C E and Passoni M 2017 Parametric investigation of laser interaction with uniform and nanostructured near-critical plasmas *Eur. Phys. J.* D **18** 202

[57] Passoni M and Lontano M 2008 Theory of light-ion acceleration driven by a strong charge separation *Phys. Rev. Lett.* **101** 115001

[58] Ferguson B and Zhang X-C 2002 Materials for terahertz science and technology *Nat. Mater.* **1** 26–33

[59] Hafez H A, Chai X, Ibrahim A, Mondal S, Frachou D, Ropagnol X and Ozaki T 2016 Intense terahertz radiation and their applications *J. Opt.* **18** 093004

[60] Ulbricht R, Hendry E, Shan J, Heinz T F and Bonn M 2011 Carrier dynamics in semiconductors studied with time-resolved terahertz spectroscopy *Rev. Mod. Phys.* **83** 543–86

[61] Chan W L, Deibel J and Mittleman D M 2007 Imaging with terahertz radiation *Rep. Prog. Phys.* **70** 1325

[62] Stojanovic N and Drescher M 2013 Accelerator- and laser-based sources of high-field terahertz pulses *J. Phys. B: At. Mol. Opt. Phys.* **46** 192001

[63] Wu Z, Fisher A S, Goodfellow J, Fuchs M, Daranciang D, Hogan M, Loos H and Lindenberg A 2013 Intense terahertz pulses from SLAC electron beams using coherent transition radiation *Rev. Sci. Instrum.* **84** 022701

[64] Ding W J, Sheng Z M and Koh W S 2013 High-field half-cycle terahertz radiation from relativistic laser interaction with thin solid targets *Appl. Phys. Lett.* **103** 204107

[65] Liao G Q *et al* 2015 Bursts of terahertz radiation from large-scale plasmas irradiated by relativistic picosecond laser pulses *Phys. Rev. Lett.* **114** 255001

[66] Liao G Q *et al* 2017 Intense terahertz radiation from relativistic laser plasma interactions *Plasma Phys. Control. Fusion* **59** 014039

[67] Tian Y, Liu J, Bai Y, Zhou S, Sun H, Liu W, Zhao J, Li R and Xu Z 2017 Femtosecond-laser-driven wire-guided helical undulator for intense terahertz radiation *Nat. Photon.* **11** 242–6

[68] Nakajima K 2017 Novel efficient THz undulator using a laser-driven wire *Light Sci. Appl.* **6** e17063

[69] Mondal S *et al* 2017 Aligned copper nanorod arrays for highly efficient generation of intense ultra-broadband thz pulses *Sci. Rep.* **7** 40058

[70] Jin Z *et al* 2016 Highly efficient terahertz radiation from a thin foil irradiated by a high-contrast laser pulse *Phys. Rev.* E **94** 033206

[71] Liao G-Q *et al* 2016 Demonstration of coherent terahertz transition radiation from relativistic laser–solid interactions *Phys. Rev. Lett.* **116** 205003

[72] Derouillat J *et al* 2017 SMILEI: a collaborative, open-source, multi-purpose particle-in-cell code for plasma simulation (arXiv:1702.05128)

[73] Gibbon P 2004 *Short Pulse Laser Interactions with Matter* (Singapore: World Scientific)